PETROGENESIS OF THE PRIMITIVE OLIVINE-PHYRIC SHERGOTTITES NORTHWEST AFRICA (NWA) 2046 AND NWA 4925. C. J. Peel[1*], G. H. Howarth[1], J.M.D. Day[2], P. le Roux[1] [1]Dept. of Geological Sciences, University of Cape Town, Cape Town, South Africa (*plxcha003@myuct.ac.za), [2]Scripps Institution of Oceanography, University of California San Diego, La Jolla, CA, USA.

Introduction: Shergottites are the most abundant and chemically diverse group of martian meteorites, and can be classified based on texture into three main groups (i.e., basaltic, olivine-phyric, poikilitic), as well as by geochemistry (i.e., based on light rare earth element [LREE] abundance, and radiogenic isotope compositions into LREE-depleted, enriched and intermediate [1-4]. LREE-depleted shergottites which display crystallization ages that range between 327 Ma and 2.4 Ga [5-7], cluster around an ejection age of 1.1 Ma years [8-9], pointing to these samples having been ejected in a single impact event. High-Resolution Imaging of impact craters on the martian surface have identified the Tharsis volcanic province as the most likely source of these depleted shergottites [10]. In this study, we present petrological and geochemical findings for two LREE-depleted olivine-phyric shergottites, Northwest Africa (NWA) 2046 and NWA 4925, to understand their evolution, as well as their relation to the LREE-depleted shergottites. We show that these meteorites broadly represent melt composition, based on bulk rock equilibrium with Mg-rich olivine.

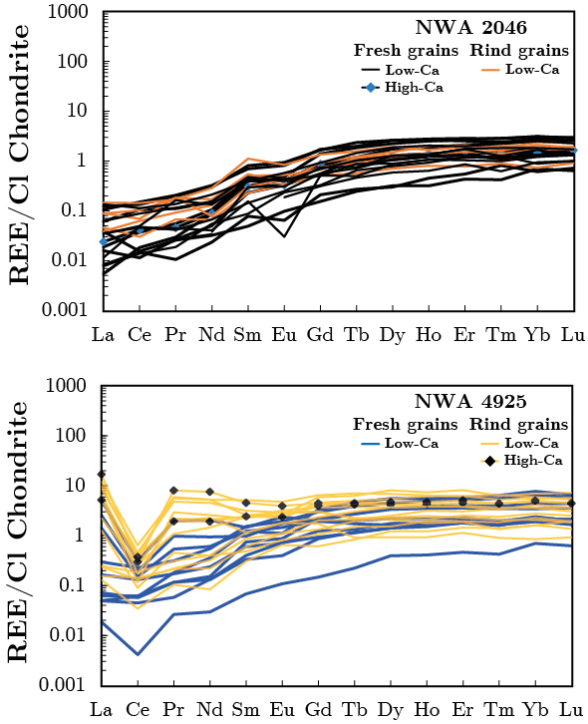

Figure 1: CI-normalized REE plots for pyroxene phenocryst from NWA 2046 and NWA 4925.

Methods: A Cameca SX-100 Microprobe analyser (University of Johannesburg, UJ) was used for in situ major and minor elemental analyses of mineral phases present in samples. Analyses were performed with beam sizes of 1-3 µm (5-10 µm on maskelynite), an accelerating voltage of 15kV and a beam current of 20nA. In situ trace element compositions for the mineral phases were analyzed using a Resolution M-50-LR Excimer laser ablation system attached to an Agilent 7500 quadrupole ICP-MS (Stellenbosch University, SU), using spot-sizes of 40-55 µm for olivine (ol), pyroxene (px) and maskelynite (mask) and 15 µm for phosphates. Small chips of each sample were analyzed at SIO for their bulk rock major and trace chemistry.

Petrography and Mineral Chemistry: Olivine megacrysts from both samples display normal zoning profiles that have a range from Fo_{83-50} (NWA 2046) and Fo_{81-48} (NWA 4925). Pyroxene grains in NWA 2046 are chemically zoned and can be separated into two distinct groups, the majority belonging to the first (type-I), which we define as having low-Ca orthopyroxene cores and augite rims. The second group of zoned pyroxene grains (type-II) have cores of clinopyroxene, either pigeonite or augite, intermediate zones of orthopyroxene and low-Ca (relative to core) pigeonite rims. The pyroxene grains in NWA 4925 are also chemically zoned, with all analyzed grains falling within the first group (type-I). Pyroxene grains in both NWA 2046 and NWA 4925 show CI-normalized LREE-depleted patterns that overlap with each other. Pyroxene in NWA 4925, however, show higher degrees of LREE enrichment and more prominent negative Ce anomalies (Fig. 1). Additionally, pyroxene grains present in the weathering rind of NWA 4925 show higher abundances of the LREE (and near-flat laying REE patterns) relative "fresh" grains, while weathering rind grains in NWA 2046 generally overlap well with "fresh" grains. Maskelynite grains in NWA 2046 show a range in composition of An_{75-62}, while those in NWA 4925 range from An_{77-66}, and are characterized by relatively flat LREE profiles with large positive Eu anomalies. Phosphates are largely merrillite with minor apatite observed. While merrillite grains are in minor abundances in both samples, they are also the major carrier of REE, and are also characterized as having LREE-depleted profiles, similar to REE profiles observed for pyroxene.

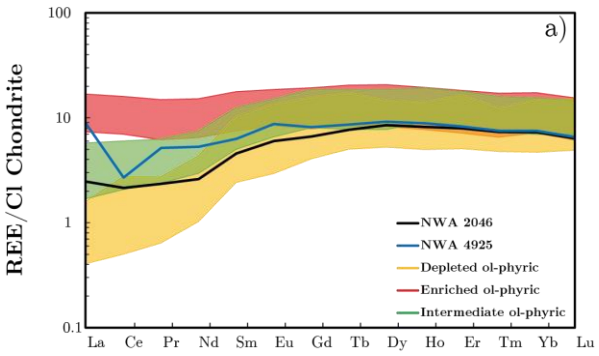

Figure 2: Bulk rock CI-normalized REE plot for NWA 2046 and NWA 4925 relative to other olivine-phyric shergottites across geochemical groups. [9 and references therein].

Whole-Rock Composition: NWA 2046 contains 16.4 wt.% MgO with a corresponding Mg# of 64, while NWA 4925 has 15.5 wt. % MgO and an Mg# of 61. Chondrite-normalized bulk-rock REE patterns for both samples show LREE-depleted profiles comparable to those of other depleted olivine-phyric shergottites (Fig. 2). NWA 2046 and NWA 4925, however, show a higher abundance of La relative to other depleted olivine-phyric shergottites.

Discussion and Conclusion: Using the K_D $^{Fe\text{-}Mg}$ for martian lavas of 0.35 [11], the most primitive olivine megacryst cores in NWA 2046 (Fo_{83}) and NWA 4925 (Fo_{81}) are in equilibrium with their respective bulk rock compositions, suggesting that these samples represent melt compositions (Fig. 3). The mineral and bulk rock REE plots for NWA 2046 and NWA 4925 all consistent with these samples being depleted olivine-phyric shergottites. In contrast with other depleted shergottites, sample NWA 2046 shows some degree of enrichment in LREE (mainly La), as well as in Sr and Ba, consistent with this sample having experienced terrestrial alteration [12-13]. Confirmation of terrestrial alternation, specifically in NWA 4925, can also be found in weathering rind pyroxene grains.

Oxygen fugacity conditions during early stages of crystallization were estimated with olivine-pyroxene-spinel [14] and V-in-olivine oxybarometry [15] calculations using six mineral assemblages from each sample. The restricted range of fO_2 for NWA 2046 using both methods span from -3.4 to -2.6 relative to the Fayalite-Magnetite-Quartz (FMQ) buffer and from -3.0 to -2.4 QFM-relative for NWA 4925, both of which overlap entirely with -2 to -4 QFM range of oxygen fugacities values calculated for LREE-depleted olivine-phyric shergottites [16-17]. When graphically compared to bulk rock $(La/Ya)_{CI}$ values, oxygen fugacity values for both NWA 2046 and NWA 4925 are shown plotting away from other depleted ol-phyric shergottites, owning to terrestrial enrichment of the LREE.

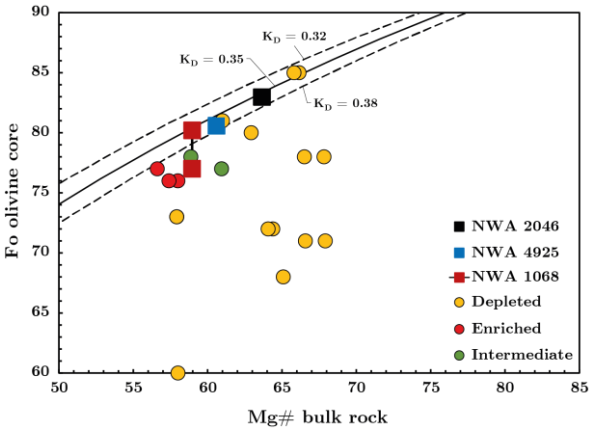

Figure 3: Bulk rock Mg# versus Forsterite content in olivine cores of olivine-phyric shergottites. Solid line represents melt-ol equilibrium $K_D^{Fe\text{-}Mg}$ value of 0.35, while the dotted lines represent the uncertainty of our solid line. (See [9] and references therein)

References: [1] Goodrich, C.A. (2002) *MAPS*, 37, B31-B34. [2] Debaille, V. (2008) *EPSL*, 269(1-2), 186-199. [3] Walton, E.L. (2012) *MAPS*, 47(9), 1449-1474. [4] McSween H.Y. (2015) *Am Min*, 100(11-12), 2380-2395. [5] Brennecka G.A. (2014) *MAPS*, 49(3), 412-418. [6] Lapen T.J. (2017) *Sci. Adv.*, 3(2), e1600922 [7] Nyquist L.E. (2001) in *Chronology and Evolution of Mars*, 96, 105-164. [8] Nishiizumi K. (2011) *LPSC 42*, abs #1608, p. 2371. [9] Udry A. (2020) JGR: Planets, 125(12). [10] Lagain A. (2021) *Nat. Commun*, 12(1), 1-9. [11] Filiberto J. *et al.* (2009) *Am Min*, 94(2-3), 256-261.[12] Crozaz G. and Wadhwa M (2001) *GCA*, 65(6), 971-977. [13] Crozaz *et al.* (2003) *GCA*, 67(24), 4727-4741. [14] Sack R.O. and Ghiorso M.S. (1991) *Contrib Mineral Petrol*, 106, 474-505. [15] Wang, J. et al. (2019) *JGR: Solid Earth*, 124(5), 4617-4638. [16] Herd C. D. K. *et al.* (2013) *LPSC* 44, abs #1719. [17] Balta, J.B. *et al.* (2015) *MAPS*, 50(1), 63-85.